Published online in Polymer Degradation and Stability, March 2017.
http://dx.doi.org/10.1016/j.polymdegradstab.2017.03.004

Consolidation Process Boundaries of the Degradation of Mechanical Properties in Compression Moulding of Natural-Fibre Bio-Polymer Composites

Hossein Mohammad Khanlou[a], Peter Woodfield[a], John Summerscales[b], Wayne Hall[a]

[a] Griffith School of Engineering, Gold Coast Campus, Griffith University, Queensland 4222, Australia
[b] Advanced Composites Manufacturing Centre, School of Marine Science and Engineering, Reynolds Building, University of Plymouth, Plymouth, Devon PL4 8AA, United Kingdom

Abstract

In spite of the volume of literature on natural fibres, bio-matrix materials and their composites, the choices of optimum process parameters such as moulding temperature, pressure and compression time are still largely based on experience, rules of thumb and general knowledge of the chemical and physical processes occurring in the melt during consolidation. The moulding process itself is a complex balance between processes that must occur for the composite to successfully consolidate and the onset of thermal degradation of the natural fibre and/or matrix materials. This paper brings together models of thermal penetration, melt infusion, thermal degradation and chemical degradation of natural polymers to construct an ideal processing window for a bio-composite. All processes are mapped in terms of normalized consolidation progress parameters making it easier to identify critical processes and process boundaries. Validation of the concept is achieved by measuring changes in the mechanical properties of a flax/PLA bio-composite formed over a range of processing conditions within and outside of the optimized window.

Keywords: Bio-polymer composites; Chemical degradation; Natural fibres; Mechanical properties; and Thermal processing degradation

1. Introduction

The use of natural fibres as the reinforcement for composites has been comprehensively reviewed by the authors of this paper [1-5] and others. One of the key challenges for the use of natural fibres for reinforcing thermoplastics and thermosets is minimizing the thermal degradation of the cellulosic material that can occur during hot processing of the composite [6]. For bio-composites, plant-derived resins such as poly (lactic acid) (PLA) and poly(L-lactic acid) (PLLA) also suffer from thermal degradation for temperatures that typically occur during the compression moulding process [7-10]. Thus the temperature and time are the key process parameters for controlling thermal degradation in both the natural fibre and the bio-based matrix material. The temperature of the hot press should be sufficiently above the melting point of the matrix to lower its viscosity and the time sufficiently long for penetration of the melt into the fibres achieving a strong bond between matrix and fibre. In competition with these requirements, the melt temperature should be as low as possible to slow the rate of thermo-chemical degradation and the time as short as possible to limit the progress of these undesired chemical reactions [7, 11]. This leaves a narrow window of opportunity to achieve

Published online in Polymer Degradation and Stability, March 2017.
http://dx.doi.org/10.1016/j.polymdegradstab.2017.03.004

a well-consolidated bio-composite without compromising the mechanical properties of matrix and fibre.

A number of studies have indicated that the moulding time has a significant effect on the mechanical properties of compression-moulded PLA-based bio-composites [12-17]. However, there is not a general consensus as to the most suitable length of time that the composite should remain at high temperature and pressure and few studies quantify the effect on the mechanical properties. Indicative process conditions from the literature are given in Table 1.

Table 1. Indicative process conditions for pressing bio-composites

Fibre	Matrix	Temperature	Pressure	Time (min)	Reference
kenaf	PLA	160 °C	10 MPa	10	[12]
cotton, lyocell, hemp, kenaf	PLA	180 °C	4.2 MPa	20	[13]
Hemp, lyocell	PLA/PP blend	195 °C	1.7 MPa	20	[14]
jute	PLA	185-195 °C	1.33 MPa	8	[15]
hemp	PLA	185 °C	2 MPa 5 MPa	5 3	[16]
40-60% nonwoven flax	PLA fibres Drying prepreg Moulding	160 °C 80 °C 180-200°C	0.4 MPa Ambient 5 MPa	5 600 5, 10 or 15	[17]

In terms of characterizing the effect of the moulding time, Alimuzzaman et al. [17] considered the effect of the moulding time on the mechanical properties of flax and PLA bio-composites using a novel air-laying process followed by hot pressing , to form a prepreg for the bio-composite. After drying the prepregs, the composites were consolidated using compression moulding. The results from their study showed small decreases in tensile and flexural strength with increasing moulding time and no measurable change to the tensile and flexural moduli. The best mechanical properties were achieved for the shortest moulding time (5 min). Neat PLA showed the same trends that were observed for the composites for strength and moduli [12].

Longer moulding times have been employed for flax fibres in other matrix materials. For example, Kumar and Anandjiwala [18] had a compression moulding time of 2 h at 170 °C for their flax – polyfurfuryl alcohol (PFA) bio-composites. Zhang et al. [19] studied the effect of process parameters on the tensile strength of flax fibre reinforced polypropylene composites they found a maximum strength for 181 °C and 45-50 min moulding time. In contrast, the

Published online in Polymer Degradation and Stability, March 2017.
http://dx.doi.org/10.1016/j.polymdegradstab.2017.03.004

effect of moulding times in excess of 30 minutes for PLA-based bio-composites does not appear to have been quantified in the literature.

While practitioners working with bio-composites are no doubt aware of the issues, there have been surprisingly few attempts to quantitatively map out the process boundaries for successful compression moulding of bio-composites. The aim of this study is to highlight the key considerations and propose a quantitative guide for moulding time limits based on the available literature and a practical study of a representative flax/PLA bio-composite.

2. Theoretical background and measures of consolidation progress

The processes occurring during manufacture of the composite can be conveniently discussed using normalized progress parameters, κ_i, where $\kappa_i = 0$ implies the process has just started and $\kappa_i = 1$ implies the process is completed or has reached a maximum or desired state. Each process parameter needs to be expressed as a function of time and temperature.

2.1 Thermal penetration and melting point

The first process after starting the hot press is to heat all the matrix to at least its melting point. Here $\kappa_{heatup} = 0$ implies the laminate is at room temperature and $\kappa_{heatup} = 1$ indicates the centre of the matrix is a melt at the set-point temperature. To achieve these limits, the progress parameter can be defined in terms of the specific enthalpy $h(T)$:

$$\kappa_{heatup} \equiv \frac{h(T_{cen}) - h_s(T_0)}{h_f(T_{platen}) - h_s(T_0)} \tag{1}$$

where T_{cen} is the temperature in the centre of the composite (i.e. half way between the two heated plattens), T_0 is the initial temperature of the composite and T_{platen} is the temperature of the platen. $h_f(T)$ is the specific enthalpy of the liquid while $h_s(T)$ is the specific enthalpy of the solid.

Evaluating $h(T_{cen})$ in Eq. (1) as a function of time requires numerical integration of the unsteady heat conduction equation including any phase change. Since this may be inconvenient, it is useful to consider two limiting cases which have analytical solutions. First, if specific heat capacity is approximately constant and the latent heat of melting can be neglected, κ_{heatup} may be approximated from a solution to the transient heat conduction equation [20]:

$$\kappa_{heatup} \approx \kappa_{sensible} \approx \frac{T_{cen} - T_0}{T_{platen} - T_0} = 1 - \frac{4}{\pi}\sum_{n=0}^{\infty}\frac{(-1)^n}{2n+1}e^{-(2n+1)^2\pi^2 at/L^2} \tag{2}$$

where a is the effective thermal diffusivity of the composite, L is the distance between the platens (i.e. the thickness of the composite) and t is time. For $\kappa_{heatup} = 0.9$, Eq. (2) gives the Fourier number:

Published online in Polymer Degradation and Stability, March 2017.
http://dx.doi.org/10.1016/j.polymdegradstab.2017.03.004

$$\frac{at}{L^2}\Big|_{\kappa=0.9} \approx 0.26 \tag{3}$$

Alternatively, if the latent heat dominates the time required for all of the matrix material to melt (i.e. the sensible heat capacity of the material is small compared with latent heat), then a second useful approximation is:

$$\kappa_{latent} \approx \sqrt{\frac{8k_{cond}\left(T_{platen}-T_m\right)t}{\left(1-V_f\right)\rho h_{fs}L^2}} \tag{4}$$

where κ_{latent} = 0 indicates all of the material is in the solid phase and κ_{latent} = 1 indicates that all of the matrix material is liquid. In Eq. (4), T_m is the melting point, k_{cond} is the effective thermal conductivity of the composite, ρ is the density of the matrix material, V_f is the volume fraction of fibre and h_{fs} the latent heat of fusion (melting). Combining Eqs. (3) and (4) a suitable approximation for the total heat up time would be:

$$t_{heatup} \approx t_{sensible} + t_{latent} \tag{5}$$

where $t_{sensible}$ is the time determined from Eq. (3) for sensible heating and t_{latent} is determined from Eq. (4) by selecting appropriate values for $\kappa_{sensible}$ and κ_{latent}. To obtain meaningful results from Eq. (4), the set-point for the platen temperature must be equal to, or greater than the melting temperature. In the literature this temperature is often identified when an endothermal peak appears in differential scanning calorimetry (DSC) curves [21]. While the melting point is usually assigned a single value, the peak normally shows some breadth which is primarily related to the size and degree of perfection of the polymer crystals [21]. The manufacturing temperature of polymeric composites is usually 20-30 °C above the melting temperature (e.g. [13-19]). This is to ensure that the viscosity of the melt is low enough to allow the PLA to flow into the pore space between the fibres during production and it allows for some variation in the melting temperature. The melting temperature of PLA is reported to be in the range of 146-152 °C in the literature [8, 22, 23] and that used in this study was measured at 148.6 °C by DSC.

Table 2 shows typical properties of PLA from previous studies [8, 22, 24] needed for evaluating the heat up and melting times from Eqs. (3) and (4). Fig. 1 shows simulated results for the time required for the progress parameters κ_{heatup} and κ_{latent} to reach 90% for different process temperatures for a PLA/flax composite with a thickness of 1 mm and fibre volume fraction V_f of 50%. For the purpose of evaluation, the effective thermal conductivity of the composite was assumed to be approximately that of PLA.

Table 2. Available data for k_{cond}, ρ, c and h_{fs} for thermal penetration

	k_{cond} (W/m.K)	ρ (kg/m^3)	c (J/kg-K)	h_{fs} (J/g)	Ref.
PLA	0.26	1260	2221	23.2	[8, 22, 24]

Published online in Polymer Degradation and Stability, March 2017.
http://dx.doi.org/10.1016/j.polymdegradstab.2017.03.004

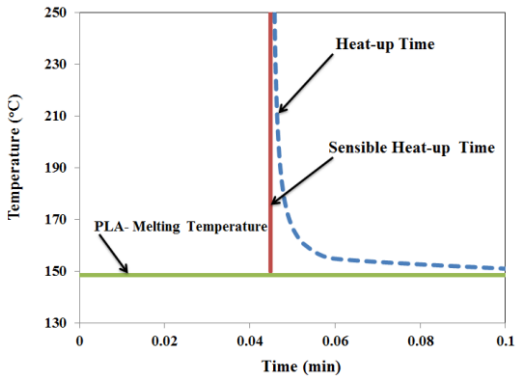

Fig. 1. Melting temperature and temperature/time maps corresponding to necessary time for fulfilling the thermal penetration times for a 1 mm thick PLA/flax composite considering both sensible heat up and time required for melting. By selecting a process temperature on this graph, the curve shows the time at that temperature required to melt 90% of the matrix (κ_{heatup} = 0.9).

In Fig. 1, the sensible heat up time (solid line) corresponds to Eq. (3) and the total heat up time (dash line) to Eq. (5). The definition of $\kappa_{sensible}$ leads to the heat up time from Eq. (3) being independent of the temperature while in Eq. (4) temperature gradients driving heat conduction through the melt are directly proportional to the temperature difference between the platen and the melting point. In either case, the heat up time is significantly less than one minute for a 1 mm thick sample. Eq. (4) indicates that the sensible heat up time is proportional to the square of the sample thickness *L*. This implies that a 10 mm thick composite will take 100 times longer to heat up than the case shown in Fig. 1.

2.2 Impregnation of matrix melt into yarn

Impregnation is a process where a polymeric matrix flows through the fibre reinforcement and completely encloses it. The dual scale impregnation process can be divided into two stages – macro impregnation (inter-tow) and micro impregnation (intra-tow) [25]. Micro-impregnation is the rate determining step where the molten thermoplastic polymer enters into the fibre yarn (or tow in the case of synthetic reinforcement) and completely wets each technical fibre. For compression moulding, by applying pressure the liquid polymer enters the yarns of twisted reinforcement fibres. In this study κ_{impreg} = 0 indicates no penetration and κ_{impreg} = 1 indicates the matrix has penetrated and completely filled the yarn, wetting each technical fibre. This model assumes the time required for macro impregnation is small in comparison to the time required for micro impregnation. To achieve these limits a progress parameter (degree of impregnation [26]) can be defined:

$$\kappa_{impreg} = \frac{A_{impreg}}{A_{yarn}} \tag{6}$$

where A_{yarn} is the cross-sectional area of a single yarn (i.e. fibre and inter-fibre porosity) and A_{impreg} is the instantaneous area within the yarn wetted by the melt. The penetration velocity can be described by Darcy's Law Eq. (7) [27]:

Published online in Polymer Degradation and Stability, March 2017.
http://dx.doi.org/10.1016/j.polymdegradstab.2017.03.004

$$\phi\vec{v} = -\frac{K_p}{\mu}\nabla P \tag{7}$$

where ∇P, μ, ϕ and K_p are the pressure gradient, viscosity of the liquid polymer matrix, the void fraction inside the tow prior to penetration and the permeability of the fibre, respectively. To obtain an estimate of the penetration time, we assume the yarn cross section is circular in shape and the unwetted region in the centre of the tow is at atmospheric pressure. In reality, the tow will be flattened out of round during compression, but this can be accounted for by using an effective radius [28]. With these assumptions, the Darcy equation gives [28, 29]

$$r\ln\left(\frac{r}{r_0}\right)\frac{dr}{dt} = \frac{K_p}{\mu\phi}\left(P_m - P_{in}\right) \tag{8}$$

where P_m is the pressure in the matrix outside of the yarn, P_{in} is the pressure in the unwetted region inside the yarn (assumed to be atmospheric pressure), r_0 is the radius of the yarn, r is the radius of the unwetted region inside the yarn. Integrating Eq. (8) and applying Eq. (6) gives the time required for reaching a required degree of impregnation as:

$$t = \frac{\phi\mu}{4K_pP_m}\left(r_0^2\kappa_{impreg} + 2\left(1-\kappa_{impreg}\right)r_0^2\ln\left(\sqrt{1-\kappa_{impreg}}\right)\right) \tag{9}$$

K_p in Eqs. (8) and (9) is a function of the microstructure of the unwetted yarn including size and connectivity of voids and technical fibre diameter. If surface wettability is neglected, K_p will be independent of fluid that passes through the porous medium [30]. Bates et al. [31] used the Carman–Kozeny equation to calculate the permeability of fibre bundles for different kinds of fibres using:

$$K_p = \frac{D_f^2}{16k_{Kozney}}\frac{\phi^3}{(1-\phi)^2} \tag{10}$$

where D_f, and k_{Konzey} are fibre diameter and the Kozney constant (which accounts for capillary, tortuosity and shape effects). Bates et al. [31] reported a range of values for k_{Konzey} and ϕ. Moreover, in compression moulding ϕ changes with pressure [29] adding considerable uncertainty in predicted values for K_p. In this study, to test the sensitivity of the model to the void fraction of the unwetted tow values, values for ϕ between 0.05 and 0.3 were used and k_{Konzey} was assumed to be 10 as a typical value [25] (see Fig. 2). The diameter of the yarn was found using optical microscopy to be 170 µm prior to composite manufacturing.

The viscosity μ of the polymer in a molten state also plays a key role in determining the impregnation process time. A number of studies have evaluated the viscosity of PLA at various temperatures in the range 170-190 °C [32-36]. The viscosity not only changes with temperature but also with the average length of the polymer molecule, i.e. with average molecular weight. However, for simplicity we have assumed that the viscosity is only a function of temperature and have fitted Eq. (11) to experimental data extracted from the study of Piyamanocha et al. [32].

$$\mu = Ce^{b/T} \tag{11}$$

Published online in Polymer Degradation and Stability, March 2017.
http://dx.doi.org/10.1016/j.polymdegradstab.2017.03.004

where *C* and *b* are empirical constants that were determined by using viscosities at two temperatures (μ = 1700 Pa.s at 170 °C and 540 Pa.s at 190 °C). Eq. (11) was used for data interpolation and extrapolation to the melting temperature line as shown in Fig. 2. Different void fractions were considered. Fig. 2 gives the time required for the penetration process to reach 90% completion (κ_{impreg} = 0.9) for any given melt temperature. Clearly from Fig. 2 the impregnation process is sensitive to the void fraction. The temperature dependence of the penetration time is due to the temperature dependence of viscosity as defined by Eq. (11). Dot points in Fig. 2 show extrapolation values at various temperatures.

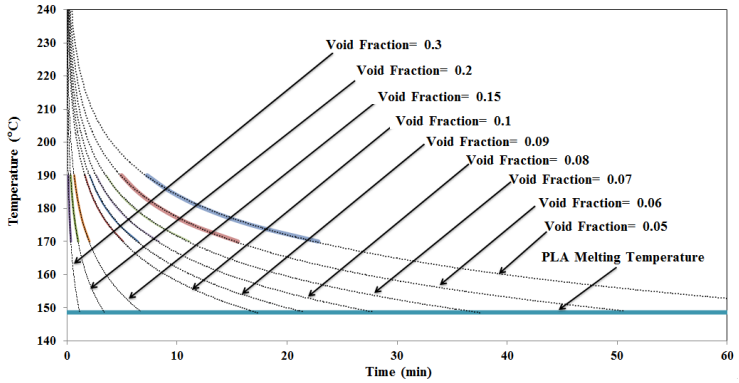

Fig. 2. Melting temperature border and Temperature/time maps corresponding to necessary time for fulfilling the impregnation process time (κ_{impreg} = 0.9) with various void fractions.

3. Theoretical background and measures of thermal degradation

Reaction progress variables α_i for degradation processes such as pyrolysis (i.e. mass-loss due to heating) are defined such that α_i = 0 for the initial state and α_i = 1 for the completely degraded state. Since degradation is a negative process, for meaningful comparison with positive (i.e. desired) consolidation processes, it may be useful to express the progress of degradation using $\kappa_i = 1 - \alpha_i$, where the desired state is κ_i = 1.

3.1 Pyrolysis and TGA data

Pyrolysis or mass loss due to high temperature heating is a common measure of thermal degradation and corresponds to a major degradation of the mechanical properties of bio-composites [37, 38]. TGA data also gives a measure of the temperature (T_{max}) at which peak loss occurs for a given heating rate. While the manufacturing temperature for compression moulding of bio-composites typically is not as high as that required for significant pyrolysis, degradation measured by mass loss can define an ultimate upper boundary for processing using data available in the literature. Moreover it is typically published using Arrhenius rate equations which are convenient for the calculations required in this study. For TGA data, the degradation progress variable α_{pyrol} is defined as:

$$\alpha_{pyrol} = \frac{m_0 - m_t}{m_0 - m_f} \tag{12}$$

Published online in Polymer Degradation and Stability, March 2017.
http://dx.doi.org/10.1016/j.polymdegradstab.2017.03.004

where m_0, m_t and m_f are the initial, at time t, and final mass of the material. Thus $\alpha_{pyrol} = 0$ indicates that no material is lost and $\alpha_{pyrol} = 1$ indicates that all potentially volatile material has gone from the material.

$$\frac{d\alpha_{pyrol}}{dt} = k\left(1-\alpha_{pyrol}\right)^n \tag{13}$$

$$k = A\exp\left(\frac{-E_a}{RT}\right) \tag{14}$$

where k determines the thermal-degradation rate, n is the order of reaction, A is the pre-exponential factor (s^{-1}), E_a is apparent activation energy, R is universal gas constant (8.3136 J/mol K) and T is temperature (K). Eqs. (13) and (14) can be integrated numerically if temperature varies with time or analytically if the temperature is constant. For the special case where $n = 1$ and T is constant:

$$\alpha_{pyrol}\big|_{n=1,T=\text{constant}} = 1-e^{-kt} \tag{15}$$

Table 3 lists various values of the A and E_a available in the literature for PLA, flax, cellulose, hemicellulose and lignin.

Table 3. Available pre-exponential constant A, energies of activation E_a, and n-order for pyrolysis

Material	*A* (s^{-1})	E_a *Overall Avg.* (kJ/mol)	*n*	*Ref.*
PLA	6.17×10^{17}	215	0.9	[38]
Flax	2.02×10^{10}	138	1	[39]
Flax*	3.50×10^{08}	121.7	1	[40]
Cellulose	3.41×10^{12}	175.6	1**	[41]
Cellulose	$10^{17.43}$	236	1	[42, 43]
Hemicellulose	1.25×10^{10}	132.9	1**	[41]
Hemicellulose	$10^{6.4}$	100	1	[42, 43]
Lignin	2.22×10^{06}	101	1**	[41]
Lignin	$10^{0.58}$	46	1	[42, 43]

* Pre-exponential A calculated from [40] (G2 trend in Fig. 4 of Ref. [40])

** Not given explicitly in original publication but assumed that the authors' intention was first order

Published online in Polymer Degradation and Stability, March 2017.
http://dx.doi.org/10.1016/j.polymdegradstab.2017.03.004

Since Eq. (14) is very sensitive to the value of E_a, large variations in the pre-exponential (e.g. as can be observed in Table 3) do not always imply large inconsistencies in mass-loss predictions over a given temperature range. Therefore, for comparing kinetic data, it is often better to calculate k and apply it to the problem of interest rather than simply compare the values of the kinetic parameters from different authors. Fig. 3 shows the time required for 10% of the volatile mass to be lost for PLA [38], flax [39], cellulose [41], hemicellulose [41] and lignin [41] at any given constant temperature. The kinetic parameters were taken from Table 3. These lines form an ultimate upper boundary for selecting a temperature for compression moulding of bio-composites.

Fig. 3 shows that hemicellulose and cellulose of natural fibre are the most sensitive and insensitive components of bio-composites respectively. Lignin requires slightly higher temperatures than hemicellulose to produce the same mass loss. Flax behaves similarly to hemicellulose and lignin for α = 0.1, which might be because the more volatile components of the flax will be lost first. For the data in Table 3, PLA requires a higher temperature than flax to achieve significant mass loss and therefore is not the main concern for the production process.

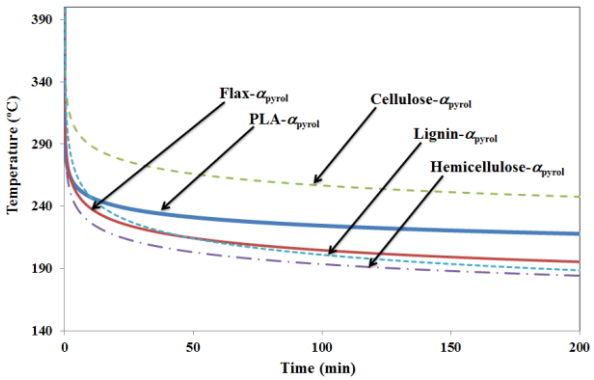

Fig. 3. Temperature/time maps corresponding to 10% mass loss (α_{pyrol} = 0.1 (i.e. κ_{pyrol} = 0.9)) for PLA, flax, cellulose hemicellulose and lignin. This figure shows the time taken for a sample of the material to lose 10% of its volatile mass for any given constant temperature.

3.2 Thermo-chemical degradation of matrix (depolymerisation via chain scission)

At temperatures lower than required for significant mass loss, chemical reactions occur within the matrix material leading to a decrease in the average length of polymer chains tending towards an equilibrium value [8-10]. Since there is strong correspondence between mechanical properties and polymer length it is appropriate to define another degradation progress parameter as:

$$\alpha_{chem-mat} = \frac{M_{n-avg}|_{t=0} - M_{n-avg}}{M_{n-avg}|_{t=0} - m_0} \tag{16}$$

where $M_{n\text{-}avg}$ is the number-average molar mass of polymers in the matrix and m_0 is the molar mass of a single monomer unit. Eq. (16) is defined such that the completely degraded state ($\alpha_{chem\text{-}mat}$ = 1) corresponds to the polymers entirely broken into monomer units. The

Published online in Polymer Degradation and Stability, March 2017.
http://dx.doi.org/10.1016/j.polymdegradstab.2017.03.004

phenomenon of random chain scission is a main mechanism for polymer thermal degradation at high temperature and is prominent in polymers with acidic end groups such as PLA [44, 45]. Here a statistical method proposed by Wachsen et al. [9] and modified by Yu et al. [10] is used to simulate changes of molar mass as a function of temperature and time. The model considers both degradation reactions and recombination reactions which occur within the polymer during the thermal processing [8-10]. Eqs. (17) and (18) describe the degradation and recombination processes respectively [10]:

$$P_n \rightarrow P_{n-r} + P_r \tag{17}$$

$$P_r + P_{n-r} \rightarrow P_n \tag{18}$$

where P_n is the polymer with a degree n of polymerization. The influence of temperature is defined using an Arrhenius law (Eqs. (19) and (20)):

$$k_d = A_d \exp(\frac{-E_{ad}}{RT}) \tag{19}$$

$$k_c = A_c \exp(\frac{-E_{ac}}{RT}) \tag{20}$$

where indexes d and c are the degradation and recombination rate indices, respectively. It is assumed that the same rate coefficients apply to polymers of any length. As expressed by Wachsen et al. [9], the concentration of a polymer of length n will be governed by:

$$\frac{d[P_n]}{dt} = -(n-1)k_d[P_n] + 2k_d\sum_{i=n+1}^{\infty}[P_i] + \frac{1}{2}k_c\sum_{i=1}^{n-1}[P_i][P_{n-i}] - k_c[P_n]\sum_{i=1}^{\infty}[P_i] \tag{21}$$

Rather than solve Eq. (21) simultaneously for a large number of polymer chains of different lengths, Yu et al. [10] re-expressed the equations in terms of moments (λ_i) of different orders which are defined according to Eq. (22) as:

$$\lambda_i = \sum_{n=1}^{\infty} n^i[P_n] \quad \text{i = 0, 1, 2, 3 ...} \tag{22}$$

The low-order moments λ_0, and λ_1 (mol/L) can be interpreted as the total number of molecules per unit volume and the total number of monomer units per unit volume (counting all monomers in all polymers), respectively. Neglecting higher-order moments, the differential equation system (Eq. (21)) reduces to [10]:

$$\frac{d\lambda_0}{dt} = k_d(\lambda_1 - \lambda_0) - \frac{k_c\lambda^2{}_0}{2} \tag{23}$$

$$\frac{d\lambda_1}{dt} = k_d(\lambda_1 - \lambda_0) \tag{24}$$

$$\frac{d\lambda_2}{dt} = \frac{k_d(\lambda_1 - \lambda_3)}{3} + k_c\lambda^2{}_1 \tag{25}$$

To close Eqs. (23)-(25), the following approximation is used [10]:

Published online in Polymer Degradation and Stability, March 2017.
http://dx.doi.org/10.1016/j.polymdegradstab.2017.03.004

$$\lambda_3 = \frac{\lambda_2}{\lambda_1 \lambda_0}[2\lambda_2\lambda_0 - \lambda^2{}_1] \tag{26}$$

Eqs. (23) to (25) require initial conditions and a means of linking the values of λ to $M_{\text{n-avg}}$ in Eq. (16). The number and weight average molar mass can be described as:

$$M_{n-avg} = m_0 \frac{\sum_{n=1}^{\infty} n[P_n]}{\sum_{n=1}^{\infty}[P_n]} = m_0 \frac{\lambda_1}{\lambda_0} \tag{27}$$

$$M_{w-avg} = m_0 \frac{\sum_{n=1}^{\infty} n^2[P_n]}{\sum_{n=1}^{\infty} n[P_n]} = m_0 \frac{\lambda_2}{\lambda_1} \tag{28}$$

where m_0 (g/mol) is the mass of an individual monomer unit. Using Eqs. (27) and (28), the polydispersity index (Q) is:

$$Q \equiv \frac{M_{w-avg}}{M_{n-avg}} = \frac{\lambda_2 \times \lambda_0}{\lambda_1{}^2} \tag{29}$$

Appropriate values of the above variables for PLA are extracted from the literature and listed in Table 4. The degradation rate is also known to be influenced by the presence of moisture [11]. Since this is not considered in the present study, the data shown in Table 4 correspond to dry PLA.

Table 4. Kinetic parameters and initial conditions for modelling polymer degradation of PLA

Ref.	A_c (L/mol/s)	E_{ac} (kJ/mol)	A_d (s^{-1})	E_{ad} (kJ/mol)	m_0 (g/mol)	$M_{n\text{-}start}$ (g/mol)	Start Q	Density (g/L)
Le Marec et al. [8]	121.6	37.7	1600	87.2	72.07	8.29×10^4	1.425	1260
Yu et al. [10]	2200	49	7.1×10^6	120	72.0	1×10^5	1.5	1260

Noting the physical meanings of λ_0 and λ_1 given above, the initial conditions for the differential Eqs. (23) to (24), can be determined from the data in Table 4 using:

$$\lambda_{0-initial} = \rho / M_{n-start} \tag{30}$$

$$\lambda_{1-initial} = \rho / m_0 \tag{31}$$

where ρ is the density of the PLA. Using the results from Eqs. (30) and (31), the initial values for λ_2 and λ_3 can be found from Eqs. (25) and (26) respectively.

For the present study, the differential Eqs. (23)-(25) were solved using a fourth-order Runge-Kutta method as recommended by Yu et al. [10]. After obtaining λ_0, λ_1 and λ_2, values of $M_{n\text{-}average}$ and $M_{w\text{-}average}$ (and subsequently $\alpha_{\text{chem-mat}}$) were determined using Eqs. (27), (28) and

Published online in Polymer Degradation and Stability, March 2017.
http://dx.doi.org/10.1016/j.polymdegradstab.2017.03.004

(16) as a function of time for different processing temperatures. The results were compared with the experimental data on molar mass degradation of PLA reported by Le Marec et al. [8] and Yu et al. [10] (not shown) to confirm that the model had been formulated correctly. Khanlou et al. [7] proposed a revised formulation of the model by Yu et al. [10] which does not require the differential Eqs. (23)-(25) and, for isothermal conditions an analytical solution is readily available.

In relation to defining process boundaries for PLA as the matrix for a bio-composite, Fig. 4 shows the time required for 10% thermal decomposition ($\alpha_{\text{chem-mat}} = 0.1$) of PLA (or PLLA in the case of Yu et al. [10]) due to thermal processing and the chain scission mechanism at various temperatures. The kinetic data by Yu et al. [10] indicates faster degradation than the data by Le Marec et al. [8] and gives a safer border to limit the zone of manufacturing process. Both degradation lines maintain a similar trend after a 100 minute interval. Since these borders are very close to melting temperature line, the chain scission mechanism for the matrix is an important consideration in the manufacturing process.

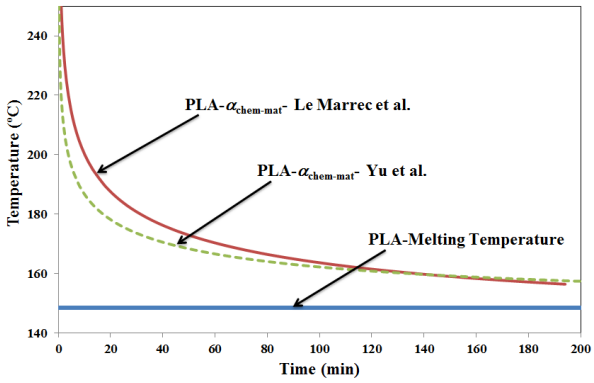

Fig. 4. Melting temperature border and Temperature/time maps corresponding to 10% chain scission ($\alpha_{\text{chem-mat}} = 0.1$ (i.e. $\kappa_{\text{chem-mat}} = 0.9$)) for PLA due to thermal processing. This figure shows the time taken for the number-average PLA polymer size to decrease by about 10% for any given constant temperature

3.3 Thermo-chemical degradation of natural fibres (Degree of polymerization of natural fibres)

Natural fibre cellulosic chains also show scission behaviour when they are exposed to a high temperature, in a similar way to polymeric matrices. To find a quantitative value for chain scission, the degree of polymerization (*DP*) (or an average number of monomeric units in a macromolecule) has been used to evaluate the degradation of natural fibres [46-49]. This is actually a dimensionless equivalent of the number-averaged molar mass ($M_{\text{n-avg}}$) since for a single polymer type, *DP* is the number-averaged molar mass divided by the molar mass of a monomer unit. Gassan et al. [47] investigated the *DP* behaviour of jute and flax fibres at various temperatures and its relationship with tenacity properties (mechanical properties) of fibre. In this study, a degradation progress parameter ($\alpha_{chem-fibre}$) is proposed to identify the chemical reaction or chain scission progress in the natural fibres with the use of *DP* as:

Published online in Polymer Degradation and Stability, March 2017.
http://dx.doi.org/10.1016/j.polymdegradstab.2017.03.004

$$\alpha_{chem-fibre} = \frac{DP\big|_{t=0} - DP}{DP\big|_{t=0} - 1} \tag{32}$$

Eq. (16) will have the same form as Eq. (32) if numerator and denominator are divided by m_0. The degree of polymerization can be determined empirically by measuring the viscosity of a natural polymer solution extracted from the fibre using a cellulose solvent [47]. Chemical rate equations are usually expressed using concentrations. For this purpose, 1/DP is proportional to the number of molecules per unit volume. For chain scission of cellulosic materials, Testa et al. [48] expressed their chemical rate equation in terms of *N* as defined in Eq. (33):

$$N = 1 - \frac{1}{DP} \tag{33}$$

For their model, a first-order kinetic rate law corresponds to the random chain scission of bonds in a linear chain polymer:

$$\frac{dN}{dt} = K \times N \tag{34}$$

Here, we have followed a similar strategy except that we have assumed that *K* is temperature-dependent according to the Arrhenius law:

$$K = A\exp(\frac{-E_a}{RT}) \tag{35}$$

For a given temperature, Eqs (34) and (35) may be solved to give:

$$t = \frac{(\ln\frac{N}{N_0})}{Ae^{-E/RT}} \tag{36}$$

where N_0 and N are $1-(1/DP_0)$ and $1-(1/(\kappa)DP_0)$, respectively, (κ=1-α) is the progress of degradation as mentioned above, and DP_0 is the initial *DP*.

Unfortunately, the necessary kinetic data for chemical degradation of flax fibre is difficult to find in the literature. In a study by Gassan et al. [47], *DP* was measured after heating flax fibre for different periods of time for three different temperatures as listed in Table 5. The initial value given for DP_0 was 1505.

Published online in Polymer Degradation and Stability, March 2017.
http://dx.doi.org/10.1016/j.polymdegradstab.2017.03.004

Table 5. *DP* of flax fibre heat treated for three time periods and at three temperatures [47]

	DP		
Time (min)	170 °C	190 °C	210 °C
40	866	509	387
120	511	360	261

For the present study, a least-squares fitting procedure was used to determine the pre-exponential factor (A = -0.178 s^{-1}) and the apparent activation energy (E_a = 50.5×10^3 J/mol) to fit Eqs. (33) to (35) to the data given in Table 5. Finally, Fig. 5 shows temperature/time maps corresponding to 10% to 90% chain scission ($\kappa_{chem\text{-}fibre}$ = 0.9 to 0.1) and was drawn in relation to defining process boundaries for flax fibre as the reinforcement for a bio-composite. This boundary corresponds to the chemical-thermal degradation of the fibre which occurs during thermal processing. This border significantly limits the zone of manufacturing process and gives a caution to the bio-composite manufacturer that the mechanical properties of bio-composite will inevitably degrade during the manufacturing process. This process boundary is of high importance to the manufacturing process in order to prevent the initial degradation during the manufacturing process.

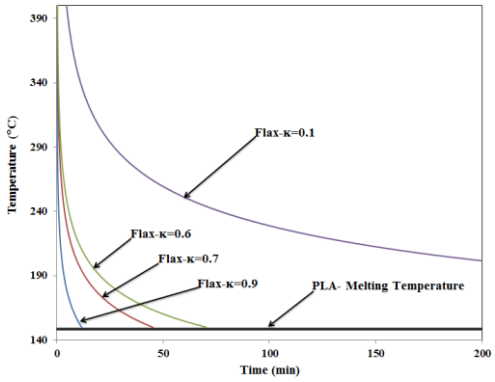

Fig. 5. Temperature/time maps corresponding to different degrees of thermo-chemical degradation of flax fibre due to thermal processing

4. Experiment for validation of concept

Ultimately we are interested in the effect that the overall process has on the mechanical properties of the composite. For this purpose, mechanical properties of a flax/PLA bio-composite were measured for different processing conditions.

4.1 Materials and methods

Unidirectional (UD) flaxply fabric (180 g/m² flax) manufactured by Lineo Company (France) was used in this study. PLA film (25 microns thick) was supplied by Magical Film Enterprises Co. Ltd. (Taiwan).

Published online in Polymer Degradation and Stability, March 2017.
http://dx.doi.org/10.1016/j.polymdegradstab.2017.03.004

Thermal transition temperatures of the PLA were measured for four samples using differential scanning calorimetry (DSC). The average glass transition temperature (T_g) was 61.9 °C and the corresponding melting temperature (T_m) was 146.2 °C.

A flat aluminium plate (3 mm thick) was treated with high temperature release agent (Aliphatic Hydrocarbones, Marbocote Ltd, UK) and used as the lower moulding surface. The top moulding surface was pre-released and attached to the upper platen of the compression moulding machine. Two layers of PLA film were placed directly on the bottom mould surface followed by a single layer of fibre and two further layers of PLA. This pattern was repeated for four composite layers. There are four layers of PLA between each reinforcement layer. The bio-composite plate was moulded with a total thickness of approximately 1 mm with a planar area of approximately 300 × 300 mm.

The compression moulding machine (Carver Inc, Wabash, USA) was set to a temperature of 170 °C which is above the melting temperature of the PLA. The bottom moulding surface and the composite layup were not introduced to the moulding machine until the top mould surface temperature reached the set point value. The composite was compressed to a pressure of 300 kPa and held at the set temperature for a set consolidation time (15, 30, 45, 60 or 120 minutes). The pressure was maintained as the top and bottom platens of the compression moulder were cooled. The cooling process was manually controlled by a supply of cold water to the platens. The temperatures of the upper and lower platens were recorded during the entire process using a data logger (USB TC-08, Pico Tech, UK) sampling at a rate of 1 Hz (Fig. 6).

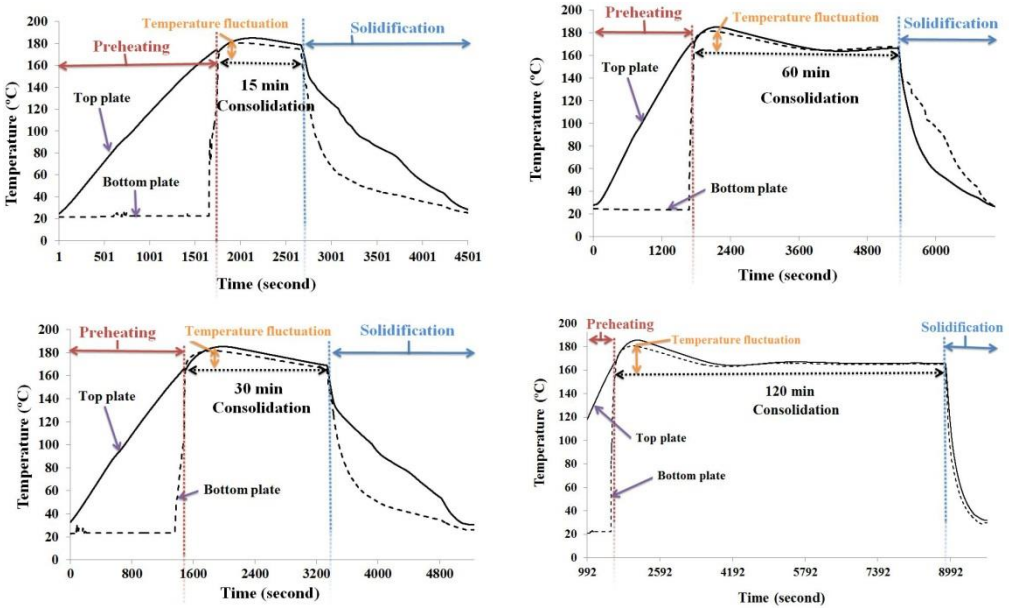

Fig. 6. Processing temperature histories for different consolidation times

Tensile test specimens were laser cut from the composite plates (parallel to the fibre direction). Sixteen samples were cut from each plate. The test specimen dimensions were 250 × 15 × 1 mm. Tensile testing was carried out using an Instron 3367 testing machine with an Instron 30 kN load cell (serial no. 68296). Gripping end tabs were used during tensile testing as recommended by ASTM D3039/D3039 M. A standard crosshead displacement rate was set at 2mm/min. The tensile strain in the specimens was measured with a 50 mm Instron

Published online in Polymer Degradation and Stability, March 2017.
http://dx.doi.org/10.1016/j.polymdegradstab.2017.03.004

extensometer attached to the surface of the material. Modulus was calculated over the axial strain range of 1000 micro-strain to 3000 micro-strain. To determine the advance estimate of the standard deviation for the flax/PLA composites, 16 tensile test specimens cut from a single plate were used.

4.2 Mechanical properties analysis

The mean mechanical properties and standard deviations for each of these times are shown in Table 6. The moduli can be seen to be fairly independent of consolidation time (means range from 20.0 to 27.0 GPa), but the tensile strength and fracture strain reduce significantly as the consolidation time increases (from 308 to 132 MPa and 2.1 to 1.2 % respectively).

Table 6. Measured mean mechanical properties of flax/PLA composites

Consolidation time [min]	Tensile Modulus [GPa] (std/CoV)	Tensile strength [MPa] (std/CoV)	Failure strain [%] (std/CoV)
15	21.1 (2.9/13%)	308 (11/3%)	2.1 (0.22/10%)
30	22.9 (1.5/6%)	280 (28/10%)	2.0 (0.22/11%)
45	27.4 (4.8/17%)	235 (32/13%)	1.2 (0.29/24%)
60	22.0 (1.8/8%)	132 (24/18%)	0.9 (0.42/46%)
120	20.1 (3.2/16%)	132 (12/9%)	1.2 (0.45/37%)

The coefficient of variation (CoV) for both modulus and failure strain increases as the consolidation time lengthens. The mean tensile strengths and fracture strains at 15 mins and 30 mins consolidation are fairly consistent (308 and 280 MPa, and 2.1 and 2.0% respectively), but decrease markedly at 60 mins and 120 mins. The tensile strength and fracture strain approximately halves when the consolidation time is $\geq$ 45 mins.

4.3 Comparison with Model

Fig. 7 shows the completed process map corresponding to the PLA/flax composite. Positive consolidation processes are assigned a value of κ = 0.9 and degradation processes α = 0.1. The experimental data for tensile strength of the composite is shown as symbols. The shaded region corresponds to the recommended processing window based on the various models. In this case, the kinetic data indicate that the upper and lower bounds for the time under the hot press are defined by thermochemical fibre degradation and melt penetration into the yarn, respectively.

Published online in Polymer Degradation and Stability, March 2017.
http://dx.doi.org/10.1016/j.polymdegradstab.2017.03.004

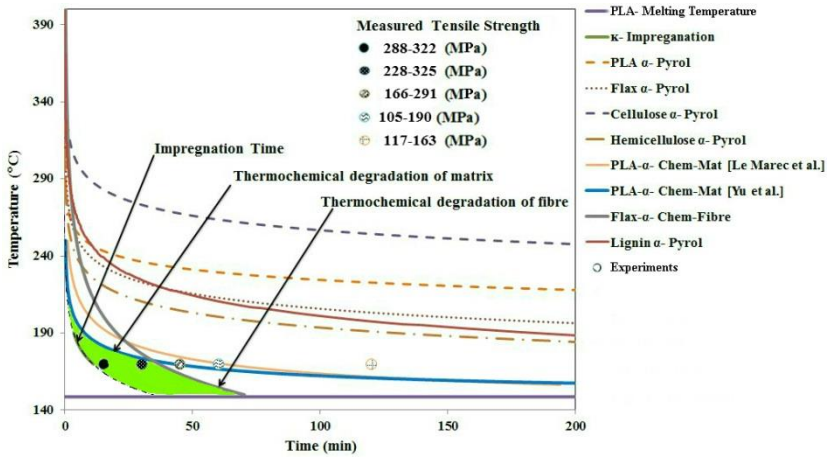

Fig. 7. Completed Temperature/time maps corresponding to κ= 0.9 or α = 0.1 and experimental data for flax/PLA bio-composite. The only exception to this is for thermo-chemical degradation of the fibre where κ= 0.6 is assigned as a compromise due to the rapid degradation of the flax fibre. The shaded region shows the range of favourable process conditions for compression moulding of this composite.

5. Conclusions

In this study we have mapped out a window of suitable temperatures and consolidation times for compression moulding of a flax-PLA bio-composite using kinetic data and available models from the literature for thermal penetration, melt-fibre impregnation and thermochemical degradation of both fibre and matrix. By expressing each of the processes using dimensionless progress variables, convenient temperature/time maps can be constructed enabling manufacturers to have an overview of degradation processes during the manufacturing process. Thus making it possible to optimize the manufacturing time, ensuring that degradation in properties of the bio-composite is minimized.

The map derived for flax/PLA composite suggests that the most important processes are penetration of the melt into the yarn which defines the minimum consolidation time and thermochemical degradation of the natural fibres which defines the maximum consolidation time allowed to avoid major degradation of the composite mechanical strength. Consistent with the model, experimental data showed a considerable reduction in tensile strength for the composite for consolidation times greater than 45 min.

Acknowledgments: The authors are grateful to Adam Parsons worked as intern with Dr Michael Heitzmann at University of Queensland for their help in DSC characterization of PLA.

Published online in Polymer Degradation and Stability, March 2017.
http://dx.doi.org/10.1016/j.polymdegradstab.2017.03.004

References

[1] J. Summerscales, N.P. Dissanayake, A.S. Virk, W. Hall, A review of bast fibres and their composites. Part 1–Fibres as reinforcements, Composites Part A: Applied Science and Manufacturing 41(10) (2010) 1329-1335.
[2] J. Summerscales, N. Dissanayake, A. Virk, W. Hall, A review of bast fibres and their composites. Part 2–Composites, Composites Part A: Applied Science and Manufacturing 41(10) (2010) 1336-1344.
[3] J. Summerscales, A. Virk, W. Hall, A review of bast fibres and their composites: Part 3–Modelling, Composites Part A: Applied Science and Manufacturing 44 (2013) 132-139.
[4] J. Summerscales, S. Grove, 7 - Manufacturing methods for natural fibre composites, Natural Fibre Composites, Woodhead Publishing2014, pp. 176-215.
[5] P.J.D. Nilmini, S. John, Life Cycle Assessment for Natural Fiber Composites, Green Composites from Natural Resources, CRC Press2013, pp. 157-186.
[6] K. Van de Velde, E. Baetens, Thermal and mechanical properties of flax fibres as potential composite reinforcement, Macromolecular Materials and Engineering 286(6) (2001) 342-349.
[7] H.M. Khanlou, W. Hall, M.T. Heitzman, J. Summerscales, P. Woodfield, Technical Note: On modelling thermo-chemical degradation of poly(lactic acid), Polymer Degradation and Stability 134 (2016) 19-21.
[8] P.E. Le Marec, L. Ferry, J.-C. Quantin, J.-C. Bénézet, F. Bonfils, S. Guilbert, A. Bergeret, Influence of melt processing conditions on poly (lactic acid) degradation: Molar mass distribution and crystallization, Polymer Degradation and Stability 110 (2014) 353-363.
[9] O. Wachsen, K. Platkowski, K.H. Reichert, Thermal degradation of poly-l-lactide—studies on kinetics, modelling and melt stabilisation, Polymer Degradation and Stability 57(1) (1997) 87-94.
[10] H. Yu, N. Huang, C. Wang, Z. Tang, Modeling of poly (L-lactide) thermal degradation: Theoretical prediction of molecular weight and polydispersity index, Journal of applied polymer science 88(11) (2003) 2557-2562.
[11] V. Taubner, R. Shishoo, Influence of processing parameters on the degradation of poly (L-lactide) during extrusion, Journal of applied polymer science 79(12) (2001) 2128-2135.
[12] S. Ochi, Mechanical properties of kenaf fibers and kenaf/PLA composites, Mechanics of materials 40(4) (2008) 446-452.
[13] N. Graupner, A.S. Herrmann, J. Müssig, Natural and man-made cellulose fibre-reinforced poly (lactic acid)(PLA) composites: An overview about mechanical characteristics and application areas, Composites Part A: Applied Science and Manufacturing 40(6) (2009) 810-821.
[14] B. Baghaei, M. Skrifvars, M. Rissanen, S.K. Ramamoorthy, Mechanical and thermal characterization of compression moulded polylactic acid natural fiber composites reinforced with hemp and lyocell fibers, Journal of Applied Polymer Science 131(15) (2014).
[15] A. Memon, A. Nakai, Fabrication and mechanical properties of jute spun yarn/PLA unidirection composite by compression molding, Energy Procedia 34 (2013) 830-838.
[16] M.A. Sawpan, K.L. Pickering, A. Fernyhough, Flexural properties of hemp fibre reinforced polylactide and unsaturated polyester composites, Composites Part A: Applied Science and Manufacturing 43(3) (2012) 519-526.
[17] S. Alimuzzaman, R.H. Gong, M. Akonda, Nonwoven polylactic acid and flax biocomposites, Polymer Composites 34(10) (2013) 1611-1619.
[18] R. Kumar, R.D. Anandjiwala, Compression-moulded flax fabric-reinforced polyfurfuryl alcohol bio-composites, Journal of thermal analysis and calorimetry 112(2) (2013) 755-760.
[19] J. Zhang, S. Li, X.M. Qian, Processing parameter optimization of flax fiber reinforced polypropylene composite, Advanced Materials Research, Trans Tech Publ, 2011, pp. 1541-1545.
[20] H.S. Carslaw, J.C. Jaeger, Conduction of heat in solids, Oxford: Clarendon Press, 1959, 2nd ed. (1959).

Published online in Polymer Degradation and Stability, March 2017.
http://dx.doi.org/10.1016/j.polymdegradstab.2017.03.004

[21] Y. Kong, J. Hay, The measurement of the crystallinity of polymers by DSC, Polymer 43(14) (2002) 3873-3878.
[22] M. Pyda, R. Bopp, B. Wunderlich, Heat capacity of poly (lactic acid), The Journal of Chemical Thermodynamics 36(9) (2004) 731-742.
[23] W. Jia, R. Gong, C. Soutis, P. Hogg, Biodegradable fibre reinforced composites composed of polylactic acid and polybutylene succinate, Plastics, Rubber and Composites 43(3) (2014) 82-88.
[24] R. Osugi, H. Takagi, K. Liu, Y. Gennai, Thermal conductivity behavior of natural fiber-reinforced composites, Proceedings of the Asian Pacific Conference for Materials and Mechanics, Yokohama, Japan, 2009, pp. 13-16.
[25] C. Mayer, X. Wang, M. Neitzel, Macro- and micro-impregnation phenomena in continuous manufacturing of fabric reinforced thermoplastic composites, Composites Part A: Applied Science and Manufacturing 29(7) (1998) 783-793.
[26] P. Peltonen, K. Lahteenkorva, E. Paakkonen, P. Jarvela, P. Tormala, The influence of melt impregnation parameters on the degree of impregnation of a polypropylene/glass fibre prepreg, Journal of Thermoplastic Composite Materials 5(4) (1992) 318-343.
[27] J. Bernhardsson, R. Shishoo, Effect of processing parameters on consolidation quality of GF/PP commingled yarn based composites, Journal of Thermoplastic Composite Materials 13(4) (2000) 292-313.
[28] W. Grouve, R. Akkerman, Consolidation process model for film stacking glass/PPS laminates, Plastics, Rubber and Composites 39(3-5) (2010) 208-215.
[29] N. Bernet, V. Michaud, P. Bourban, J. Manson, An impregnation model for the consolidation of thermoplastic composites made from commingled yarns, Journal of Composite Materials 33(8) (1999) 751-772.
[30] M. Lagardère, C.H. Park, S. Panier, Permeability of natural fiber reinforcement for liquid composite molding processes, Journal of Materials Science 49(18) (2014) 6449-6458.
[31] P. Bates, D. Taylor, M. Cunningham, Compaction and transverse permeability of glass rovings, Applied Composite Materials 8(3) (2001) 163-178.
[32] P. Piyamanocha, T. Sedlacek, P. Sáha, On pressure and temperature affected shear viscosity behaviour of Poly (Lactid) acid melt, Recent Researches in Geography, Geology, Energy, Environment and Biomedicine-Proc. of the 4th WSEAS Int. Conf. on EMESEG'11, 2nd Int. Conf. on WORLD-GEO'11, 5th Int. Conf. on EDEB'11, 2011.
[33] S.-Y. Gu, K. Zhang, J. Ren, H. Zhan, Melt rheology of polylactide/poly (butylene adipate-co-terephthalate) blends, Carbohydrate polymers 74(1) (2008) 79-85.
[34] D. Shumigin, E. Tarasova, A. Krumme, P. Meier, Rheological and mechanical properties of poly (lactic) acid/cellulose and LDPE/cellulose composites, Materials Science 17(1) (2011) 32-37.
[35] K. Hamad, M. Kaseem, F. Deri, Melt rheology of poly (lactic acid)/low density polyethylene polymer blends, Advances in Chemical Engineering and Science 1(04) (2011) 208.
[36] H.J. Lehermeier, J.R. Dorgan, Melt rheology of poly (lactic acid): Consequences of blending chain architectures, Polymer Engineering & Science 41(12) (2001) 2172-2184.
[37] S. Pilla, Handbook of bioplastics and biocomposites engineering applications, John Wiley & Sons2011.
[38] G. Wang, A. Li, Thermal Decomposition and Kinetics of Mixtures of Polylactic Acid and Biomass during Copyrolysis, Chinese Journal of Chemical Engineering 16(6) (2008) 929-933.
[39] A. Arbelaiz, B. Fernández, J.A. Ramos, I. Mondragon, Thermal and crystallization studies of short flax fibre reinforced polypropylene matrix composites: Effect of treatments, Thermochimica Acta 440(2) (2006) 111-121.
[40] K. Van De Velde, P. Kiekens, Thermal degradation of flax: The determination of kinetic parameters with thermogravimetric analysis, Journal of Applied Polymer Science 83(12) (2002) 2634-2643.

Published online in Polymer Degradation and Stability, March 2017.
http://dx.doi.org/10.1016/j.polymdegradstab.2017.03.004

[41] L. Gašparovič, J. Labovský, J. Markoš, L. Jelemenský, Calculation of kinetic parameters of the thermal decomposition of wood by distributed activation energy model (DAEM), Chemical and Biochemical Engineering Quarterly 26(1) (2012) 45-53.
[42] L. Burhenne, J. Messmer, T. Aicher, M.-P. Laborie, The effect of the biomass components lignin, cellulose and hemicellulose on TGA and fixed bed pyrolysis, Journal of Analytical and Applied Pyrolysis 101 (2013) 177-184.
[43] M.G. Grønli, G. Varhegyi, C. Di Blasi, Thermogravimetric analysis and devolatilization kinetics of wood, Industrial & Engineering Chemistry Research 41(17) (2002) 4201-4208.
[44] M. Gupta, V. Deshmukh, Thermal oxidative degradation of poly-lactic acid, Colloid and Polymer Science 260(5) (1982) 514-517.
[45] Y. Doi, Y. Kanesawa, M. Kunioka, T. Saito, Biodegradation of microbial copolyesters: poly (3-hydroxybutyrate-co-3-hydroxyvalerate) and poly (3-hydroxybutyrate-co-4-hydroxybutyrate), Macromolecules 23(1) (1990) 26-31.
[46] G. Arifuzzaman Khan, S. Shahrear Palash, M. Shamsul Alam, A. Chakraborty, M. Gafur, M. Terano, Isolation and characterization of betel nut leaf fiber: Its potential application in making composites, Polymer Composites 33(5) (2012) 764-772.
[47] J. Gassan, A.K. Bledzki, Thermal degradation of flax and jute fibers, Journal of Applied Polymer Science 82(6) (2001) 1417-1422.
[48] G. Testa, A. Sardella, E. Rossi, C. Bozzi, A. Seves, The kinetics of cellulose fiber degradation and correlation with some tensile properties, Acta polymerica 45(1) (1994) 47-49.
[49] G. Jiang, W. Huang, L. Li, X. Wang, F. Pang, Y. Zhang, H. Wang, Structure and properties of regenerated cellulose fibers from different technology processes, Carbohydrate Polymers 87(3) (2012).